Health and Place 57 (2019) 305–312

Contents lists available at ScienceDirect

Health & Place

journal homepage: www.elsevier.com/locate/healthplace

The natural environment and birth outcomes: Comparting 3D exposure metrics derived from LiDAR to 2D metrics based on the normalized difference vegetation index

Geoffrey H. Donovan[a,*], Demetrios Gatziolis[a], Kristen Jakstis[b], Saskia Comess[c]

[a] USDA Forest Service, PNW Research Station, 620 SW Main, Suite 502, Portland, OR 97205, USA
[b] University of Freiburg, Faculty of Environmental and Natural Resources, Tennenbacher Straße 4, D- 79106 Freiburg, Germany
[c] Yale University, Department of Environmental Health Sciences, 60 College Street, New Haven, CT 65520, USA

1. Introduction

Numerous studies have shown that exposure to the natural environment is associated with a range of improved health outcomes including reduced mortality (Mitchell and Popham, 2008), improved birth outcomes (Hystad et al., 2014; Laurent et al., 2013), lower incidence of cancer (James et al., 2016), better mental health (Alcock et al., 2014; Kuo and Faber Taylor, 2004), improved respiratory health (Donovan et al., 2018; Liddicoat et al., 2018), and lower rates of cardiovascular disease (Donovan et al., 2013; Tsao et al., 2014). The majority of these greenness-and-health studies have characterized exposure to the natural environment using the normalized difference vegetation index (NDVI), which is a greenness index, bounded by −1 and 1, that is typically derived from satellite imagery. This reliance on NDVI is understandable. It is available globally and has been collected consistently for decades, so it can be used to measure change over time. In addition, some NDVI measures (notably those based on Landsat imagery) are available at no cost. However, NDVI also has significant limitations. It has coarse resolution (typically 5–30 m) and is two dimensional, so it may do a poor job of characterizing exposure to the natural environment especially in urban areas that have highly heterogeneous vegetation.

Advances in remote sensing mean that future greenness-and-health studies need not rely on NDVI. In particular, the increasing availability of Light Detection and Ranging imagery (LiDAR) will allow future studies to use higher-resolution, 3D green metrics. Whether these more sophisticated measures provide any additional insight into the relationship between the natural environment and public health is, however, unclear. We address this question by estimating the relationship between exposure to the natural environment and birth outcomes using two different types of exposure metrics: one set derived from LiDAR and the other derived from 30 m-resolution Landsat imagery.

1.1. Literature review

The link between the natural environment and birth outcomes is perhaps the most studied greenness-and-health relationship. Donovan et al. (2011) examined the relationship between the natural environment and birth outcomes in Portland, Oregon (n = 5696). Using 1 m-resolution classified aerial imagery, they found that women with more tree cover within 50 m of their homes were less likely to have a small for gestational age (SGA) birth.

Most subsequent studies of greenness and birth outcomes characterized exposure to the natural environment using 30 m-resolution NDVI derived from Landsat imagery (Agay-Shay et al., 2014; Dadvand et al., 2012; Grazuleviciene et al., 2015; Hystad et al., 2014; Laurent et al., 2013; Markevych et al., 2014). These studies all found a positive association between NDVI and birth weight in buffers ranging from 50 m to 500 m around maternal address. In addition, two of the studies (Dadvand et al., 2012; Laurent et al., 2013) found that this relationship was strongest for women with low levels of education.

Two studies examined the relationship between the natural environment and birth outcomes using 250 m-resolution NDVI derived from Moderate Resolution Imaging Spectroradiometer (MODIS) data. Casey et al. (2016) found that greenness in 250 m and 1,250 m buffers around maternal address was associated with a reduced probability of SGA and pre-term birth for 20,569 children born in Pennsylvania. Similarly, in a large cohort (n = 3,026,603) of children born in Texas, Cusack et al. (2017) found that greenness within 250 m of maternal address was positively associated with birth weight, although this relationship was markedly attenuated by controlling for SES.

Not all greenness-and-birth-outcomes studies used NDVI. Ebisu et al. (2016) characterized exposure to the natural environment using 30 m-resolution National Land Cover Data, which categorizes all land in the US into 1 of 20 classes. In a large cohort of children born in Connecticut (n = 239,811), the authors found that more green land cover was positively associated with birth weight.

* Corresponding author.
E-mail addresses: gdonovan@fs.fed.us (G.H. Donovan), dgatziolis@fs.fed.us (D. Gatziolis), k.jakstis@gmail.com (K. Jakstis), saskia.comess@yale.edu (S. Comess).

https://doi.org/10.1016/j.healthplace.2019.05.011
Received 14 November 2018; Received in revised form 5 May 2019; Accepted 13 May 2019
1353-8292/ Published by Elsevier Ltd.

Finally, not all studies found a significant relationship between exposure to the natural environment and birth outcomes. In a cohort of 61,140 children born in Rhode Island, Glazer et al. (2018) found that 30 m-resolution NDVI in a 500 m buffer around maternal address was positively associated with birth weight. This result was robust to adjustment for individual-level SES but became insignificant after adjusting for neighborhood-level SES. This result is consistent with other studies that found that the relationship between greenness and birth outcomes is attenuated by controlling for SES (Cusack et al., 2017).

The use of NDVI to characterize exposure to the natural environment is not confined to birth-outcome studies. For example, previous studies have used NDVI to examine the relationship between greenness and cognitive development (Dadvand et al., 2015), mortality (James et al., 2016), and asthma (Donovan et al., 2018).

1.2. LiDAR metrics

Airborne Laser Scanning (ALS) is an active remote-sensing technology that uses short pulses of light emitted from LiDAR instruments to illuminate targets of interest. Pulse photons pass through the atmosphere, hit the target and are backscattered. A portion of these backscattered photons are intercepted by the LiDAR sensors. Differences in pulse return times, combined with precisely recorded aircraft location and altitude, yield 3D representations of targeted scenes. Pulses oriented towards opaque objects, such as roads, bare ground, or buildings, typically generate a single point or return. In contrast, non-solid objects, including tree crowns, can generate multiple returns from a single pulse (for a detailed introduction to ALS and LiDAR see Gatziolis and Andersen (2008)). Raw LiDAR data are inherently three-dimensional and comprise a dense cloud of points with precise location information. Conversely, the information content of the satellite imagery used to calculate NDVI is two dimensional.

ALS is the preferred method for generating detailed and precise digital descriptions of ground surfaces (Liu, 2008), in part because of its ability to penetrate non-solid objects. In wildland settings, ALS data applications include hydrologic modeling (Barber et al., 2005), assessment of forest above-ground biomass (Sheridan et al., 2014), and mapping of snow depth (Deems et al., 2013). In urban settings, LiDAR has been used to delineate road networks (Soilán et al., 2018), detect impervious surfaces (Weng, 2012), and to measure individual trees (Höfle et al., 2012).

The resolution, and cost, of LiDAR data depends on its acquisition specifications, including pulse density (quantified as number of pulses per unit area) and overall spatial extent. Higher pulse densities produce higher-resolution imagery but require the plane acquiring the LIDAR to fly at a lower altitude and to substantially overlap adjacent scan lines, which results in an increase in flight time and cost. Large scan angles widen the scan swath and can reduce cost but can also cause problems, because LiDAR is most accurate when the laser pulse is close to perpendicular to the ground (directly under the aircraft). Artifacts proliferate as the scan angle diverges from the perpendicular, especially in areas with complex topography.

2. Methods

2.1. Data and study area

Our study area is 403 km^2 on the Westside of the Portland, Oregon Metropolitan Area (Fig. 1) that incorporates parts of Portland, Beaverton, and Hillsboro. LiDAR was acquired over the study area between December 29, 2012 and January 2, 2013 at eight pulses per square meter, which generated an average of 2.20 ground returns per square meter. The diameter of the laser pulse at ground level was 30 cm, so the entire target area was effectively illuminated (i.e. census rather than sampling). Fig. 2 shows a perspective view of the LiDAR point cloud for an example scene in the study area.

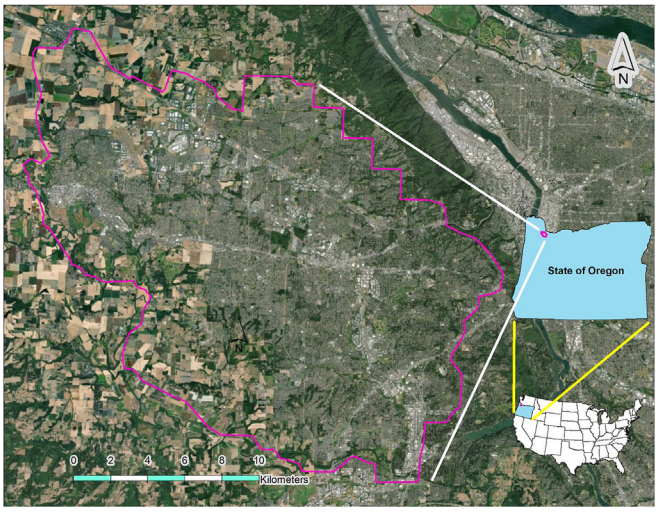

Fig. 1. Study area on the Westside of the Portland Metropolitan Area.

Fig. 2. Perspective view of the high-density ALS point cloud in Portland, Oregon Metropolitan Area.

2.2. Outcomes

We obtained data on birth outcomes from the Oregon Health Authority's Center for Health Statistics. From 2008 to 2014, there were 14,682 singleton live births in our study area. We defined a birth as small for gestational age (SGA) if the baby's weight was below the 15th percentile based on gestational age and gender (Xu et al., 2010) (we did not calculate race-specific thresholds). Our reference population for defining SGA births was all US births in 2009 and 2010 (Talge et al., 2014). We defined births that occurred before 37 weeks gestational age as preterm and births that occurred before 32 weeks gestational age as very preterm. This study was approved by the Oregon Health Authority (#RRC180046) and Yale University's IRB (#2000023085).

2.3. Exposure metrics

Fig. 3 shows an example of a LiDAR-point cloud along with 2D representations of vegetation height derived from the LiDAR data at different spatial resolutions. To convert the raw LiDAR data into exposure metrics, we first classified all returns as either vegetation, built, or other (water, for example) using a module in the GlobalMapper 20 software package. Next, we created a 1-m resolution landcover raster over the entire study area by calculating the frequency of LiDAR return classes and assigning the majority class to each cell. We ensured that the resolution and coordinate origin of the landcover classification raster matched the one of the Digital Terrain Model (DTM) (description of the ground surface) provided by the LiDAR data vendor. This co-

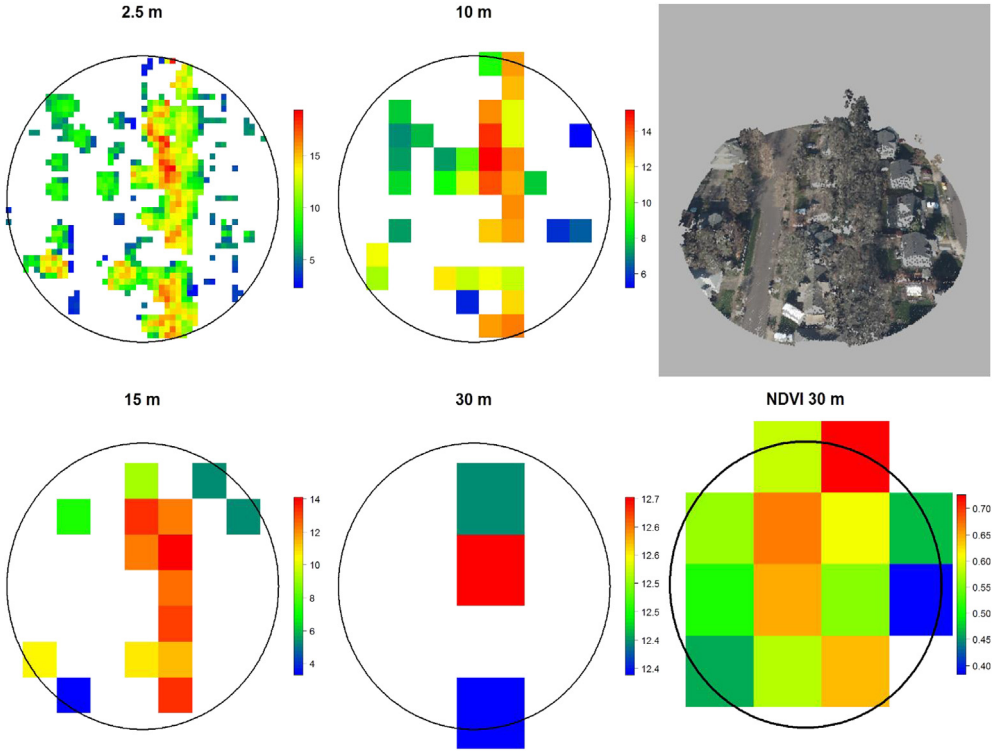

Fig. 3. LiDAR-derived representation of mean vegetation height at different spatial resolution, perspective view of corresponding point cloud, and satellite imagery-derived NDVI raster in the study area.

registration of the landcover classification raster and the DTM guaranteed there would be no degradation of precision in class assignments when the two were used together to discriminate between land-cover types. We used near-neighbor interpolation and class-majority rules to calculate land-cover rasters with progressively coarser resolution: 2.5, 5, 10, 15, and 30 m. For raster cells classified as vegetation we calculated five metrics using only returns classified as vegetation: maximum vegetation height, 90th percentile of vegetation height, mean of vegetation height, standard deviation of vegetation height, and mean vegetation entropy. Entropy is a unit-less metric derived from the raw LiDAR point cloud, which quantifies the variability in the position of the points within the cloud. A landscape consisting of very dense mature, even-aged deciduous trees would have a low entropy value, because most of the returns would be near the top of the canopy. In contrast, a landscape consisting of some tall trees mixed with understory vegetation would have a high entropy value.

Fig. 4 shows four of these metrics for an example plot (60 m buffer with 5 m resolution). For clarity, we did not include 90th percentile of vegetation height, as its distribution was almost identical to the distribution of maximum of vegetation height.

We next calculated the mean value of these five metrics in 60, 120, and 240 m buffers around the centroid of each house's lot and the proportion of each buffer covered by vegetation. We chose buffer sizes that were multiples of 30 to make our measures compatible with 30 m-resolution NDVI metrics. For each class of metric—maximum vegetation height, for example—we created 15 variables (three buffer sizes and five resolutions). Finally, we calculated mean NDVI in 60 m, 120 m, and 240 m buffers around each address using a 30 m, satellite-imagery-based NDVI base layer following the process detailed in Chander et al. (2009) and retrieved from Google Earth Engine for year 2012 (Gorelick et al., 2017).

To allow odds ratios on NDVI and LiDAR metrics to be easily compared, we standardized all continuous exposure metrics by subtracting the mean and dividing by the standard deviation.

2.4. Covariates

We obtained data on covariates from birth records including gender, plurality, parity, maternal medical complications and health characteristics (including tobacco and alcohol use, hypertension and diabetes), congenital anomalies, maternal and paternal demographic characteristics, prenatal care, method of payment for birth, and maternal residential address.

2.5. Statistical analysis

We used a two-step process to estimate logit models of SGA, preterm, and very preterm births accounting for exposure to greenness and controlling for covariates. First, we use an iterative backwards selection, with progressively smaller p-value thresholds (final threshold $p < 0.1$), to estimate a model without variables describing exposure to the natural environment (the backwards selection process was done by hand not using an automated process). To this base model, we systematically added different green metrics to determine the influence of buffer size, resolution, and different underlying imagery. To help with model selection, we calculated Aikaike Information Criterion (AIC) for each model. In addition, we estimated linear versions of each model in which the dependent variable was either birthweight or gestational age (results not shown). This allowed us to calculate variance-inflation factors (VIF) for each independent variable. If VIFs revealed multicollinearity, we either dropped the problematic variable or created composite variables. In particular, tree height and the standard deviation of tree height are highly correlated, and we wanted to include both in a single model, because the landscape-architecture literature has shown that people prefer heterogeneous natural landscapes with both tall vegetation but also open areas (de Val et al., 2006; Wang and Zhao, 2017). Neither vegetation height, nor variation in vegetation height, alone would adequately describe these sort of landscapes. To address this issue, we created four indicator variables that denoted whether vegetation height, and the standard deviation of vegetation height,

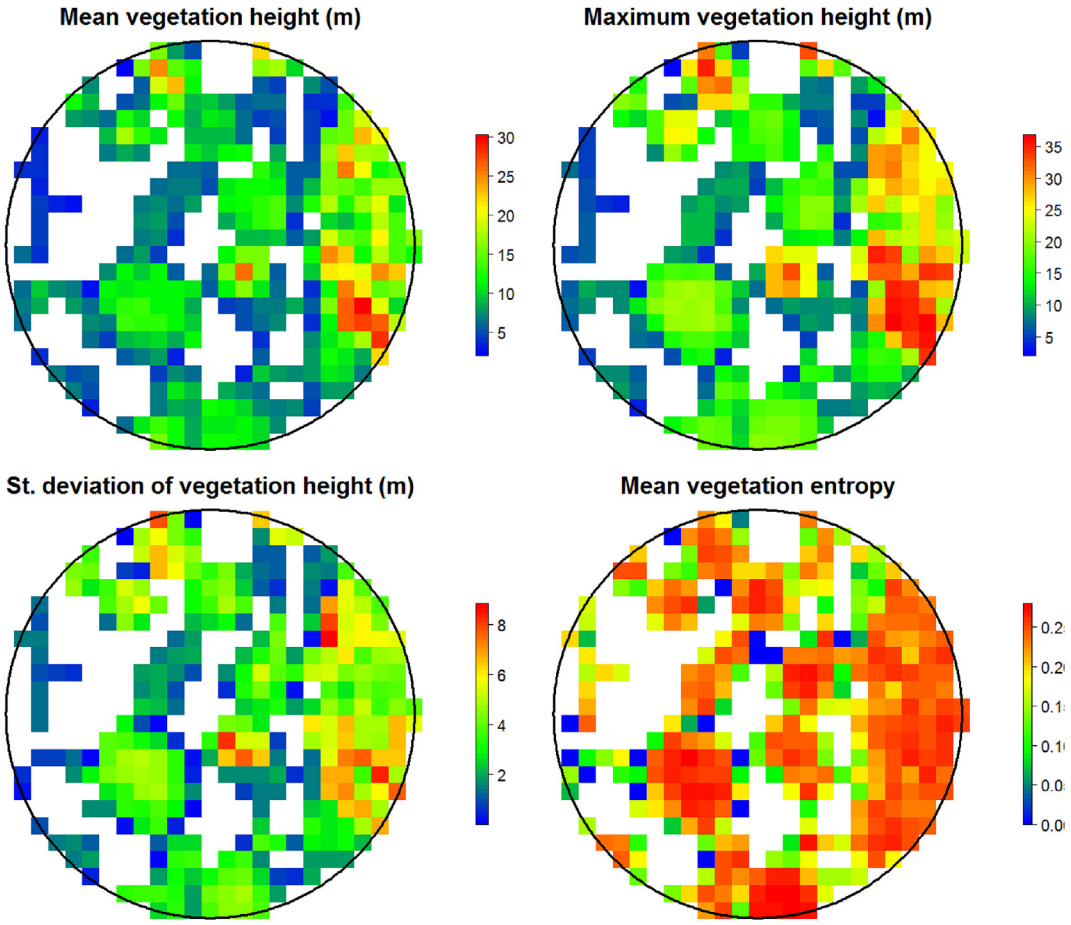

Fig. 4. Example of LiDAR-derived vegetation metrics within a 60-m circular buffer in the study area, displayed at 5-m raster resolution. .

were above or below their mean values. For example, a buffer was classified as high-high, if the mean of vegetation height was above its mean value (across all buffers of the same size and resolution) and the standard deviation of vegetation height was also above its mean value. In contrast, we classified a buffer as low-low, if mean vegetation height and the standard deviation of vegetation height were both below their respective mean values. For convenience, we refer to these indicators as landscape-type indicators. Supplementary Figs. 1–4 are short videos showing examples of each of the four landscape types. We chose to split vegetation height and standard deviation into only two categories (thereby creating four landscape types) for two reasons. First, splitting vegetation height and standard deviation into more categories would have created statistical-power problems. For example, even with just four landscapes types, only 5% of landscapes in our analysis were in the low-high class. Second, as the number of landscape classes increased, results would have been increasingly difficult to interpret.

Supplementary video related to this article can be found at https://doi.org/10.1016/j.healthplace.2019.05.011.

Insignificant variables can still be confounders (Rothman et al., 2008), so we systematically reintroduced insignificant variables paying particular attention to those that theory, or past studies, suggest may by associated with birth weight. If a reintroduced variable induced a 10% of larger change in coefficients of interest, then we retained it.

3. Results

The results for non-green variables were consistent with past research and *a priori* expectations. Note that birth year was a risk factor for SGA birth, indicating that SGA births became more common later in the study period (see Table 1).

The mean of vegetation height (2.5 m resolution and 60 m buffer) was protective of SGA birth (Table 2). This result is consistent with previous research in Portland, which found that trees in a 50 m buffer were protective of SGA birth (Donovan et al., 2011). None of the green metrics were protective of preterm or very preterm birth, which was again consistent with previous research.

Characterizing exposure to the natural environment using four landscape-indicator variables modestly improved the fit of the model (Table 2). In particular, the two landscape types for which the standard deviation of vegetation height was above average were protective of SGA birth. Low-high landscapes were the most protective (OR: 0.775, 95% CI: 0.602–0.996) followed by high-high landscapes (OR: 0.854, 95% CI: 0.764–0.954). Although low-high landscapes were more protective than high-high landscapes, the statistical significance of this relationship was lower than for high-high landscapes. This may be an issue of statistical power: only 5.0% of landscapes were classified as low-high, whereas 37% of landscapes were classified as high-high. Entropy, which also measures vegetation heterogeneity, was not significantly associated with either SGA or preterm birth.

Fig. 5 shows that the magnitude and statistical significance of the landscape-type indicator variables declined as buffer size increased. The impact of changing resolution was less systematic, although there was some loss of significance as resolution coarsened (Fig. 6).

NDVI was also protective of SGA birth, although the NDVI model did not perform as well as the two models that used LiDAR metrics (Table 2). For reference, the base SGA model, without any green metrics, had a McFadden R^2 of 0.0266 and an AIC of 10,435.

Table 1
Descriptive statistics for select exposures and covariates for children born in the study area 2008–2012 (n = 14,682).

Variable	Mean	Standard deviation
Birth weight (g)	3371	576
Gestational age (weeks)	39	1.9
Birth order	2.0	1.1
Obese (%)	19	39
Overweight (%)	24	43
Underweight (%)	3.7	19
Tobacco use during pregnancy (%)	5.7	23
Payment: private insurance (%)	68	46
Payment: public insurance (%)	28	45
Mother's race: white (%)	82	38
Mother's race: Pacific Islander (%)	1.2	11
Mother's race Asian (%)	13	34
Mother's race: Native American (%)	1.6	13
Mother's race: black (%)	2.9	17
Mother's race: Hispanic (%)	23	42
Mean of maximum tree height (m) 60 m buffer	11.5	3.7
Mean of maximum tree height (m) 120 m buffer	12.3	3.5
Mean of maximum tree height (m) 240 m buffer	13.2	3.1
Mean of 90th percentile of tree height (m) 60 m buffer	10.6	3.2
Mean of 90th percentile of tree height (m) 120 m buffer	11.4	3.5
Mean of 90th percentile of tree height (m) 240 m buffer	12.1	3.7
Mean of mean tree height (m) 60 m buffer	8.2	2.6
Mean of mean tree height (m) 120 m buffer	8.7	2.5
Mean of mean tree height (m) 240 m buffer	9.3	2.3
Entropy 60 m buffer	0.62	0.044
Entropy 120 m buffer	0.63	0.035
Entropy 240 m buffer	0.64	0.025
Vegetation 60 m buffer (%)	29.4	45.5
Vegetation 120 m buffer (%)	30.0	45.8
Vegetation 240 m buffer (%)	30.1	45.9
NDVI 60 m	0.50	0.086
NDVI 120 m	0.52	0.076
NDVI 240 m	0.53	0.067

4. Discussion

We created multiple metrics describing exposure to the natural environment and tested which best explained the likelihood of an SGA birth in a cohort of children born in the Portland, Oregon Metropolitan Area between 2008 and 2014. Metrics derived from LiDAR, and those based on 30 m-resolution NDVI data, were both protective of SGA birth. However, regression models with LiDAR metrics performed the best and revealed unique information about the relationship between the natural environment and birth outcomes. Specifically, we found that increased vegetation height was protective of SGA births. In addition, we found that variation in vegetation height was protective of SGA births. This relationship would not have been revealed by NDVI metrics, as they rely on 2D imagery that contains no information about vegetation height.

Results suggest increased vegetation height is protective of SGA births, but that the greatest protection comes from landscapes with both high vegetation and also variation in vegetation height. In contrast, homogenous landscapes such as grass fields (low-low landscape) or dense forests (high-low landscape) were not protective. However, the insignificance of low-low landscapes could be partly because these landscapes may be more likely to contain built landscape elements like roads or parking lots (binary metrics take into account vegetation height and variation in vegetation height, but they do not account for the total area covered by vegetation).

Our finding that heterogeneous landscapes offer the most protection against SGA birth is consistent with the broader landscape-architecture literature that has repeatedly found that people prefer heterogeneous natural landscapes. For example, Wang and Zhao (2017) assessed the landscape preferences of respondents using a series of photographs. Homogenous landscapes, that were either very open or very closed, had the lowest ratings. Similarly, de Val et al. (2006) found that structural heterogeneity was an important determinant of landscape preference.

The protective effect of heterogeneous vegetation height may provide some insight into the mechanisms linking the natural environment and birth outcomes. In particular, it is unlikely that the natural environment exerts its protective effect predominantly through

Table 2
Logit regression results for small-for-gestational age birth (weight < 15 percentile) with three different measures of exposure to the natural environment: mean of mean tree height (60 m buffer and 2.5 m resolution), indicator variable denoting whether tree height and tree SD are above average (60 m buffer and 2.5 m resolution), and NDVI (60 m buffer and 30 m resolution).

	3D METRICS (CONTNUOUS)		*3D METRICS (BINARY)*		*NDVI*	
VARIABLES	OR	CI	OR	CI	OR	CI
Mother's race: Hispanic (%)	1.288***	1.118–1.483	1.290***	1.120–1.485	1.269***	1.101–1.463
Mother's race: black (%)	1.818***	1.389–2.379	1.806***	1.380–2.363	1.792***	1.369–2.346
Mother's race: Native American (%)	1.120	0.760–1.650	1.120	0.760–1.650	1.113	0.755–1.640
Mother's race Asian (%)	2.051***	1.791–2.349	2.048***	1.789–2.345	2.060***	1.799–2.360
Mother's race: Pacific Islander (%)	0.777	0.465–1.300	0.774	0.463–1.295	0.776	0.464–1.297
Mother's race: Other (%)	1.056	0.742–1.503	1.054	0.740–1.500	1.057	0.743–1.505
Payment: public insurance (%)	1.166**	1.025–1.327	1.167**	1.026–1.328	1.148**	1.008–1.307
Payment: self-pay (%)	0.675*	0.424–1.073	0.670*	0.421–1.067	0.670*	0.421–1.067
Payment: other (%)	1.017	0.457–2.266	1.011	0.454–2.252	1.018	0.457–2.266
Tobacco use during pregnancy (%)	1.632***	1.335–1.995	1.649***	1.348–2.016	1.635***	1.338–1.999
Underweight (%)	1.720***	1.387–2.134	1.717***	1.384–2.130	1.712***	1.380–2.124
Overweight (%)	0.778***	0.683–0.887	0.777***	0.682–0.886	0.775***	0.680–0.884
Obese (%)	0.727***	0.626–0.844	0.723***	0.623–0.840	0.724***	0.623–0.840
Birth order	0.861***	0.818–0.906	0.862***	0.820–0.908	0.863***	0.820–0.908
Birth year	1.097**	1.015–1.187	1.100**	1.017–1.189	1.098**	1.015–1.187
Mean of tree height (60 m buffer, 2.5 m resolution)	0.929***	0.880–0.981				
Height high, SD of height low (60 m buffer, 2.5 m resolution)			0.932	0.717–1.212		
Height low, SD of height high (60 m buffer, 2.5 m resolution)			0.775**	0.602–0.996		
Height high, SD of height high (60 m buffer, 2.5 m resolution)			0.854***	0.764–0.954		
NDVI (60 m)					0.944**	0.896–0.995
McFadden R2	0.0272		0.0275		0.027	
AIC	10,429		10,431		10,433	
Observations	14,677		14,682		14,682	

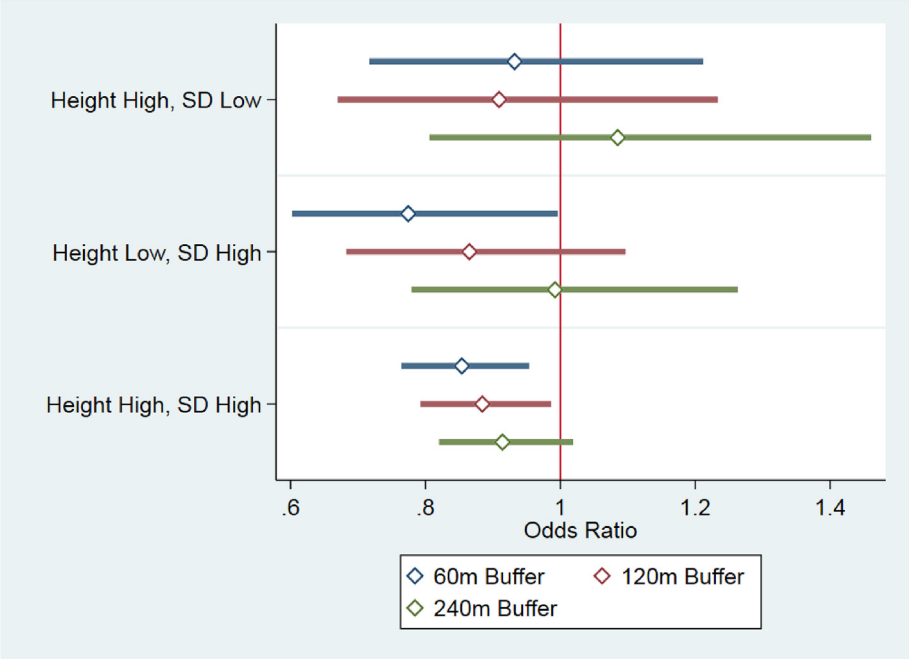

Fig. 5. Odds-ratio plots for landscape-type indicators (60, 120, and 240 m).

improvements in air quality. If that were the case, then we would expect landscape types with greater leaf area (high-low, for example) to be most protective. There are number of mechanisms that may explain the observed protective effect of landscape types. Perhaps, the most plausible is that aesthetically pleasing landscape types reduce stress and are psychologically restorative (Kaplan, 1995; Li and Sullivan, 2016). In addition, it is possible that heterogeneous landscapes may encourage people to spend more time outdoors thereby promoting social connectivity, and increased social connectivity is associated with improvements in a broad range of health outcomes (Cacioppo and Cacioppo, 2014).

We are not suggesting that LiDAR should entirely replace NDVI as a source of exposure metrics in greenness-and-health studies. For international or country-wide studies, NDVI is one of the few available data sources for characterizing exposure to the natural environment. In addition, despite NDVI being a coarse 2D exposure metric, it was significantly associated with the probability of an SGA birth, and the results from the NDVI and LiDAR models were broadly consistent. Nonetheless, future studies may wish to supplement NDVI with LiDAR metrics, as LiDAR may reveal unique information about the relationship between the natural environment and the health outcome under study.

LiDAR acquisitions can be costly and are often funded by a consortium of interested groups. However, raw and derived data for many of these acquisitions are freely available and cover an increasing area.

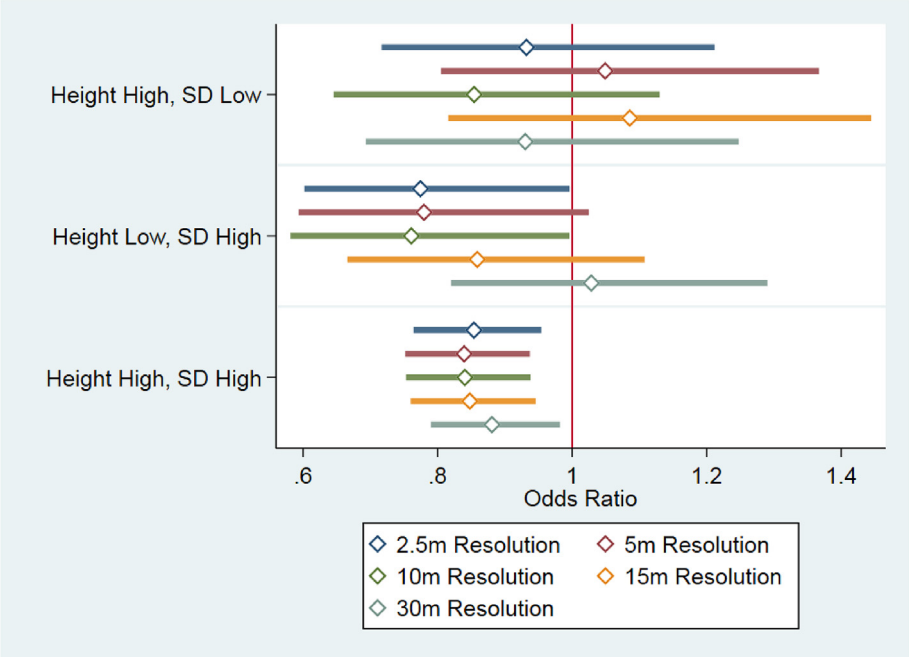

Fig. 6. Odds-ratio plots for landscape-type indicators (2.5, 5, 10, 15, and 30 m resolution).

For example, in Oregon, where this study was conducted, 40% of forested areas have been scanned with high-density LiDAR once, and several places have been flown repeatedly. As well as cost and data-availability considerations, analyses involving LiDAR data can be more complex and computationally intensive than working with 2D satellite data.

Technological advancements in active remote-sensing technologies such as ALS continue to improve data information content and reduce cost. For example, recently commercialized single-photon and Geiger-mode ALS systems (Stoker et al., 2016) offer an order of magnitude higher return density for a fraction of the cost of the standard discrete-return systems, as they can be operated from higher above-ground altitudes and aircraft speeds.

We found that regression models using LiDAR-derived metrics modestly out performed equivalent models that used NDVI-derived metrics. More importantly, results from the two models support distinctly different policy prescriptions. The NDVI model suggests that simply adding more greenness will protect against SGA. However, the NDVI model provides no insight into the best form this additional greenness should take. In contrast, the LiDAR model suggests that the structural arrangement of this greenness matters. Simply adding more greenness may not always be protective (the coefficient on high-low landscapes was insignificant, for example). To be most effective, additional greenness should increase vertical heterogeneity.

Current policy goals for increasing vegetation in urban areas may have been influenced by the limitations of exposure metrics including NDVI. For example, many US cities (including the ten largest) have explicit tree-planting goals (Donovan, 2017). Virtually all of these goals are stated in terms of planting a certain number of trees (New York City's Million-Tree Initiative, for example) or increasing canopy cover (Portland, Oregon plans to expand canopy cover from 30% to 33%). Simple tree-planting targets—such as “Let's plant a million trees”—are easily understood goals that may galvanize public support. “Let's increase the standard deviation of mean vegetation height by 0.1” is, perhaps, less compelling. Nonetheless, if our results are confirmed, then more nuanced policy goals may be appropriate.

Our study has several limitations. LiDAR allowed us to characterize aspects of the natural environment that had not been captured by extant 2D imagery. However, LiDAR does have limitations. It cannot determine vegetation species, for example. In addition, the algorithms we used to classify a return as vegetation, building, or other were imperfect and resulted in several notable artifacts. For example, the edges of buildings were often misclassified as vegetation, because when a LiDAR pulse obliquely hits the side of a building, it can generate multiple returns that the algorithm mistakes for non-solid vegetation (these artifacts can be seen in Supplementary Figs. 1–4). In addition, measuring the physical extent of the natural environment is only one component of exposure. People with exactly the same vegetation around their homes may interact with it in markedly different ways. Therefore, to be most effective, LiDAR may need to be combined with other technologies (location data from smart phones, for example) to better characterize a person's exposure to the natural environment. It is also unknown whether our results hold in other locations or for other health outcomes. Finally, this was an observational study that couldn't establish a causal relationship between greenness and the birth outcomes. In particular, it is possible that more appealing landscape types are associated with other drivers of adverse birth outcomes. Nonetheless, we believe that our results demonstrate that LiDAR data can be used to reveal unique information about the relationship between the natural environment and health.

Funding sources

This study was partially supported by two endowments from the Yale University School of Public Health: the A. J. Stolwijk Fellowship Award and the Climate Change & Health Initiative.

Appendix A. Supplementary data

Supplementary data to this article can be found online at https://doi.org/10.1016/j.healthplace.2019.05.011.

References

Agay-Shay, K., Peled, A., Crespo, A.V., Peretz, C., Amitai, Y., Linn, S., Friger, M., Nieuwenhuijsen, M.J., 2014. Green spaces and adverse pregnancy outcomes. Occup. Environ. Med. 71, 562–569.
Alcock, I., White, M.P., Wheeler, B.W., Fleming, L.E., Depledge, M.H., 2014. Longitudinal effects on mental health of moving to greener and less green urban areas. Environ. Sci. Technol. 48, 1247–1255.
Barber, C.P., Shortridge, A.J.C., Science, G.I., 2005. Lidar elevation data for surface hydrologic modeling: resolution and representation issues. 32, 401–410.
Cacioppo, J.T., Cacioppo, S., 2014. Social relationships and health: the toxic effects of perceived social isolation. Soc. Personal. Psychol. Compass 8, 58–72.
Casey, J.A., James, P., Rudolph, K.E., Wu, C.-D., Schwartz, B., 2016. Greenness and birth outcomes in a range of Pennsylvania communities. Int. J. Environ. Res. 13, 311.
Chander, G., Markham, B.L., Helder, D.L., 2009. Summary of current radiometric calibration coefficients for Landsat MSS, TM, ETM+, and EO-1 ALI sensors. Remote Sens. Environ. 113, 893–903.
Cusack, L., Larkin, A., Carozza, S., Hystad, P.J.E.r., 2017. Associations between Residential Greenness and Birth Outcomes across Texas, vol. 152. pp. 88–95.
Dadvand, P., Nazelle, A.d., Figuearas, F., Basagaña, X., Su, J., Amoly, E., Jerret, M., Vrijheid, M., Sunyer, J., Nieuwenhuijsen, M.J., 2012. Green space, health inequality and pregnancy. Environ. Int. 44, 3–30.
Dadvand, P., Nieuwenhuijsen, M.J., Esnaola, M., Forns, J., Basagana, X., Alvarez-Pedrerol, M., Rivas, I., Lopez-Vicente, M., De Castro Pascual, M., Su, J., Jerrett, M., Querol, X., Sunyer, J., 2015. Green spaces and cognitive development in primary schoolchildren. Proc. Natl. Acad. Sci. USA 112, 7937–7942.
de Val, G.d.l.F., Atauri, J.A., de Lucio, J.V., 2006. Relationship between landscape visual attributes and spatial pattern indices: a test study in Mediterranean-climate landscapes. Landsc. Urban Plan. 77, 393–407.
Deems, J.S., Painter, T.H., Finnegan, D.C., 2013. Lidar measurement of snow depth: a review, J. Glaciol. 59, 467–479.
Donovan, G.H., 2017. Including public-health benefits of trees in urban-forestry decision making. Urban For. Urban Green. 22, 120–123.
Donovan, G.H., Butry, D.T., Michael, Y.L., Prestemon, J.P., Liebhold, A.M., Gatziolis, D., Mao, M.Y., 2013. The relationship between trees and human health: evidence from the spread of the emerald ash borer. Am. J. Prev. Med. 44, 139–145.
Donovan, G.H., Gatziolis, D., Longley, I., Douwes, J., 2018. Vegetation diversity protects against childhood asthma: results from a large New Zealand birth cohort. Native Plants 4, 358–364.
Donovan, G.H., Michael, Y.L., Butry, D.T., Sullivan, A.D., Chase, J.M., 2011. Urban trees and the risk of poor birth outcomes. Health Place 17, 390–393.
Ebisu, K., Holford, T.R., Bell, M.L., 2016. Association between greenness, urbanicity, and birth weight. Sci. Total Environ. 542, 750–756.
Gatziolis, D., Andersen, H.-E., 2008. A Guide to LIDAR Data Acquisition and Processing for the Forests of the Pacific Northwest. US Department of Agriculture, Forest Service, Pacific Northwest Research Station, OR, pp. 32 Gen. Tech. Rep. PNW-GTR-768.
Glazer, K.B., Eliot, M.N., Danilack, V.A., Carlson, L., Phipps, M.G., Dadvand, P., Savitz, D.A., Wellenius, G.A., 2018. Residential green space and birth outcomes in a coastal setting. Environ. Res. 163, 97–107.
Gorelick, N., Hancher, M., Dixon, M., Ilyushchenko, S., Thau, D., Moore, R., 2017. Google Earth engine: planetary-scale geospatial analysis for everyone. Remote Sens. Environ. 202, 18–27.
Grazuleviciene, R., Danileviciute, A., Dedele, A., Vencloviene, J., Andrusaityte, S., Uždanaviciute, I., Nieuwenhuijsen, M.J., 2015. Surrounding greenness, proximity to city parks and pregnancy outcomes in Kaunas cohort study. Int. J. Hyg Environ. Health 218, 358–365.
Höfle, B., Hollaus, M., Hagenauer, J., Sensing, R., 2012. Urban vegetation detection using radiometrically calibrated small-footprint full-waveform airborne LiDAR data, J. Photogrammetry. 67, 134–147.
Hystad, P., Davies, H.W., Frank, L., Van Loon, J., Gehring, U., Tamburic, L., Brauer, M., 2014. Residential greenness and birth outcomes: evaluating the influence of spatially correlated built-environment factors. Environ. Health Perspect. 122, 1095–1102.
James, P., Hart, J.E., Banay, R.F., Laden, F., 2016. Exposure to greenness and mortality in a nationwide prospective cohort study of women. Environ. Health Perspect. 124, 1344–1352.
Kaplan, S., 1995. The restorative benefits of nature: toward an integrative framework. J. Environ. Psychol. 15, 169–182.
Kuo, F.E., Faber Taylor, A., 2004. A potential natural treatment for attention-deficit/hyperactivity disorder: evidence from a national study. Am. J. Public Health 94, 1580–1586.
Laurent, O., Wu, J., Li, L., Milesi, C., 2013. Green spaces and pregnancy outcomes in Southern California. Health Place 24, 190–195.
Li, D., Sullivan, W.C., 2016. Impact of views to school landscapes on recovery from stress and mental fatigue. Landsc. Urban Plan. 148, 149–158.
Liddicoat, C., Bi, P., Waycott, M., Glover, J., Lowe, A.J., Weinstein, P., 2018. Landscape biodiversity correlates with respiratory health in Australia. J. Environ. Manag. 206, 113–122.
Liu, X., 2008. Airborne LiDAR for DEM generation: some critical issues. Prog. Phys. Geogr. 2, 31–49.

Markevych, I., Fuertes, E., Tiesler, C.M., Birk, M., Bauer, C.P., Koletzko, S., von Berg, A., Berdel, D., Heinrich, J., 2014. Surrounding greenness and birth weight: results from the GINIplus and LISAplus birth cohorts in Munich. Health Place 26, 39–46.
Mitchell, R., Popham, F., 2008. Effects of exposure to natural environment on health inequalities: an observational population study. Lancet 372, 1655–1660.
Rothman, K.J., Greenland, S., Lash, T.L., 2008. Modern Epidemiology, third ed. Wolters Kluwer, Philadelphia, PA.
Sheridan, R.D., Popescu, S.C., Gatziolis, D., Morgan, C.L., Ku, N.-W.J.R.S., 2014. Modeling forest aboveground biomass and volume using airborne LiDAR metrics and forest inventory and analysis data in the Pacific Northwest. 7, 229–255.
Soilán, M., Truong-Hong, L., Riveiro, B., Laefer, D., 2018. Automatic extraction of road features in urban environments using dense ALS data. Int. J. Appl. Earth Observ. 64, 226–236.
Stoker, J.M., Abdullah, Q.A., Nayegandhi, A., Winehouse, J.J.R.S., 2016. Evaluation of single photon and geiger mode lidar for the 3D elevation program. 8, 767.
Talge, N.M., Mudd, L.M., Sikorskii, A., Basso, O.J.P., 2014. United States Birth Weight Reference Corrected for Implausible Gestational Age Estimates. pp. 2013–3285 peds.
Tsao, T.M., Tsai, M.J., Wang, Y.N., Lin, H.L., Wu, C.F., Hwang, J.S., Hsu, S.H., Chao, H., Chuang, K.J., Chou, C.C., Su, T.C., 2014. The health effects of a forest environment on subclinical cardiovascular disease and heath-related quality of life. PLoS One 9, e103231.
Wang, R., Zhao, J., 2017. Demographic groups' differences in visual preference for vegetated landscapes in urban green space. Sustain. Cities Soc. 28, 350–357.
Weng, Q., 2012. Remote sensing of impervious surfaces in the urban areas: requirements, methods, and trends. Remote Sens. Environ. 117, 34–49.
Xu, H., Simonet, F., Luo, Z.C., 2010. Optimal birth weight percentile cut-offs in defining small- or large-for-gestational-age. Acta Paediatr. 99, 550–555.